Journal of Alloys and Compounds 509 (2011) 1590–1594

Contents lists available at ScienceDirect

Journal of Alloys and Compounds

journal homepage: www.elsevier.com/locate/jallcom

Isothermal section of the Co–Er–Y ternary system at 500 °C

Wei He[a,b,*], Yongzhi Zhang[a,b], Yunhong Zhao[a,b], Lingmin Zeng[a,b]

[a] Key Laboratory of Nonferrous Metal Materials and New Processing Technology, Ministry of Education (Guangxi University), Nanning 530004, PR China
[b] College of Materials Science and Engineering, Guangxi University, Nanning 530004, PR China

ARTICLE INFO

Article history:
Received 22 April 2010
Received in revised form 25 October 2010
Accepted 28 October 2010
Available online 9 November 2010

Keywords:
Co–Er–Y system
Phase diagram
X-ray diffraction

ABSTRACT

The isothermal section of the phase diagram of the Co–Er–Y ternary system at 500 °C was investigated by X-ray powder diffraction technique, differential thermal analysis, scanning electron microscopy with energy dispersive analysis and optical microscopy. The 500 °C isothermal section consists of 14 single-phase regions, 19 two-phase regions, and 6 three-phase regions. Six pairs of corresponding compounds Er_2Co_{17} and Y_2Co_{17}, Er_2Co_7 and Y_2Co_7, $ErCo_3$ and YCo_3, $ErCo_2$ and YCo_2, Er_4Co_3 and Y_4Co_3, Er_3Co and Y_3Co and metals Y and Er form a continuous series of solid solutions. The maximum solid solubility of Y in the compounds $Er_{12}Co_7$ is about 19 at.% Y.

1. Introduction

R–Co (R = rare earth elements) compounds have been received a lot of attention because some intermetallic compounds in the R–Co systems show outstanding permanent magnetic properties. For instance, RCo_5 and R_2Co_{17} are permanent magnetic materials. Investigations on the binary systems of Co–Er, Co–Y and Er–Y have been found in literature [1–5]. It was reported that there are eight intermetallic compounds existing in the Co–Er system, i.e., Er_2Co_{17}, $ErCo_5$, Er_2Co_7, $ErCo_3$, $ErCo_2$, Er_4Co_3, $Er_{12}Co_7$, and Er_3Co [2]. There are 12 binary compounds reported in the Y–Co binary system, i.e., Y_2Co_{17}, YCo_5, Y_2Co_7, YCo_3, YCo_2, Y_2Co_3, Y_6Co_7, YCo, Y_4Co_3, Y_3Co_2, Y_8Co_5 and Y_3Co [1]. However, the reports on some Co–Y compounds, i.e., YCo_5, Y_2Co_3, Y_6Co_7, Y_4Co_3, Y_3Co_2 and Y_8Co_5 were inconsistent in previous investigations [1,3–9]. Buschow [6,7] pointed out that the compounds YCo_5 and $ErCo_5$ decomposed by eutectoid reaction $RCo_5 \leftrightarrow R_2Co_{17} + R_2Co_7$ at 750 °C and 1200 °C, respectively. However, Ray [8] reported that it is uncertain whether eutectoid reaction would have really occurred in the RCo_5 phases at low temperature for Y and other light rare-earth elements (La to Gd). The compound Y_4Co_3 was described to be Y_9Co_7 in Ref. [9], and instead of Y_4Co_3, Y_9Co_7 was reported to exist in Ref. [3]. Grover et al. [9] indicated that the phase Y_3Co_2 broke down rapidly to yield the Y_9Co_7 phase after any annealing. Nevertheless, Wu et al. [3] stated that the Y_3Co_2 phase did not decomposed when annealed at 550 °C and 650 °C for 1 h but decomposed to Y_8Co_5 and Y_9Co_7 when annealed at 700 °C for the same time. Some investigations on the Co–R(1)–R(2) systems are reported in literature [10–14]. However, no investigation on the phase diagram of the Co–Er–Y ternary system is available in literature. The purpose of this work is to study systematically the phase relations of the Co–Er–Y ternary system at 500 °C.

2. Experimental

Samples with 2 g each were prepared by arc-melting of initial materials of at least of 99.9 wt.% purity under high-purity argon atmosphere. The samples were turned over and remelted three times to ensure good homogeneity. The weight loss is less than 0.5% for all alloy buttons. The as-cast samples were sealed in vacuum quartz tubes and annealed for homogenization treatment. The homogenization temperatures were chosen on the basis of the binary phase diagrams of the Er–Co, Y–Co and Er–Y systems and the result of differential thermal analysis (DTA) of some typical ternary alloys. The samples with Co concentration larger than 66.7 at.% were vacuum annealed at 900 °C for 30 days, the others were at 600 °C for 40 days. The samples were cooled down to 500 °C at a rate of 50 °C/day and kept at 500 °C for 7 days, and finally quenched into liquid nitrogen. For the electron probe microanalysis and metallographic analysis of the samples, standard techniques were used. The metallographic samples were etched by a solution with a ratio of $1HF:3HNO_3:500H_2O$.

The X-ray diffraction data were collected on a Rigaku D/Max 2500PC diffractometer with CuK_α radiation and graphite monochromator operated at 40 kV, 200 mA. Phase analysis of the samples was performed by using computer software JADE5.0 [15] applied to the JCPDS-ICDD Powder Diffraction File (PDF) database (ICDD, 2002 release). Differential thermal analysis (DTA) was performed on a Netzsch STA 409PC thermal analysis meter. Scanning electron microscopy (SEM, Hitachi S-3400N) with energy dispersive analysis (EDS, EDAX) and optical microscopy were used for microstructural analysis.

* Corresponding author at: College of Materials Science and Engineering, Guangxi University, 100 Daxue Road, Nanning, Guangxi 530004, PR China. Tel.: +86 771 327 5918; fax: +86 771 323 9406.
E-mail addresses: elsawh@126.com, wei_he@gxu.edu.cn (W. He).

0925-8388/$ – see front matter © 2010 Elsevier B.V. All rights reserved.
doi:10.1016/j.jallcom.2010.10.174

3. Results and discussion

3.1. Phase analysis

In the Er–Co and Y–Co systems, all the binary compounds have been confirmed to exist at 500 °C except $ErCo_5$ and YCo_5. The X-ray diffraction patterns of these compounds basically corresponded with the respective PDF data or the diffraction patterns calculated from the crystallographic data available in literature by using the PowderCell program.

Samples with composition near $ErCo_5$ and YCo_5 were prepared. The binary compounds $ErCo_5$ and YCo_5 were not observed at 500 °C under our experimental conditions. This is in good agreement with Refs. [2,6,7]. The samples with compositions near the composition line $Y_{1-x}Er_xCo_5$ consisted of the only two phases of $Er_{2-x}Y_xCo_{17}$ and $Er_{2-x}Y_xCo_7$. Fig. 1 presents the XRD pattern of the sample no. B12 ($Co_{80}Er_3Y_{17}$) indicating that the sample consisted of $Er_{2-x}Y_xCo_7$ and $Er_{2-x}Y_xCo_{17}$. This indicated that the phase $Y_{1-x}Er_xCo_5$ decomposed into $Er_{2-x}Y_xCo_{17}$ and $Er_{2-x}Y_xCo_7$ under this heat treatment condition. XRD pattern of the non-equilibrated sample no. 61 ($Co_{83.3}Er_1Y_{15.7}$) consisting of the phases of YCo_5 and Y_2Co_{17} shows clearly the existence of the phase YCo_5 in the sample, as shown in Fig. 2 (the sample contained small amount of Y_2O_3 and Er_2O_3). The DTA measurement also supports the decomposition reaction ($YCo_5 \leftrightarrow Y_2Co_{17} + Y_2Co_7$) occurred near 805 °C. This decomposition

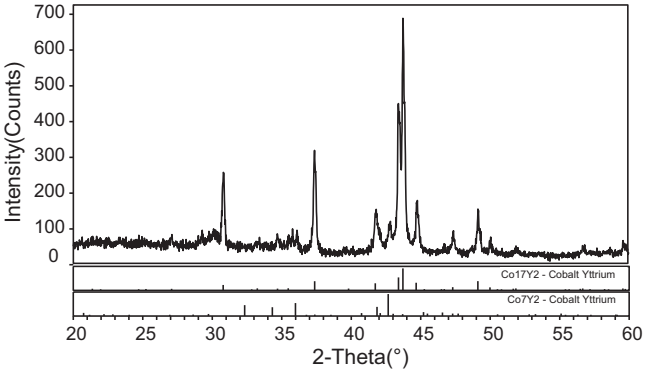

Fig. 1. XRD patterns of the sample no. B12 ($Co_{80}Er_3Y_{17}$) consisting of the phases of $Er_{2-x}Y_xCo_{17}$ and $Er_{2-x}Y_xCo_7$.

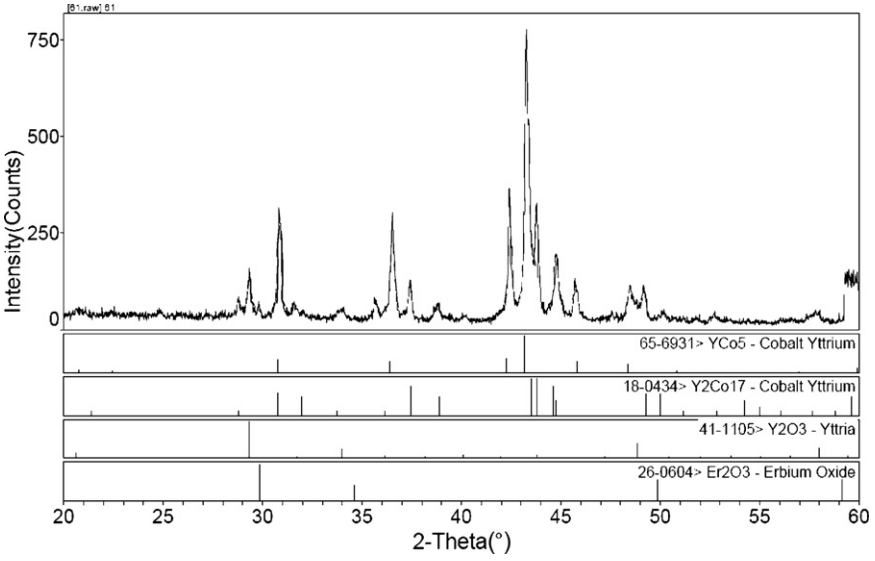

Fig. 2. XRD pattern of the non-equilibrated sample no. 61 ($Co_{83.3}Er_1Y_{15.7}$) consisting of the phases of YCo_5 and Y_2Co_{17}.

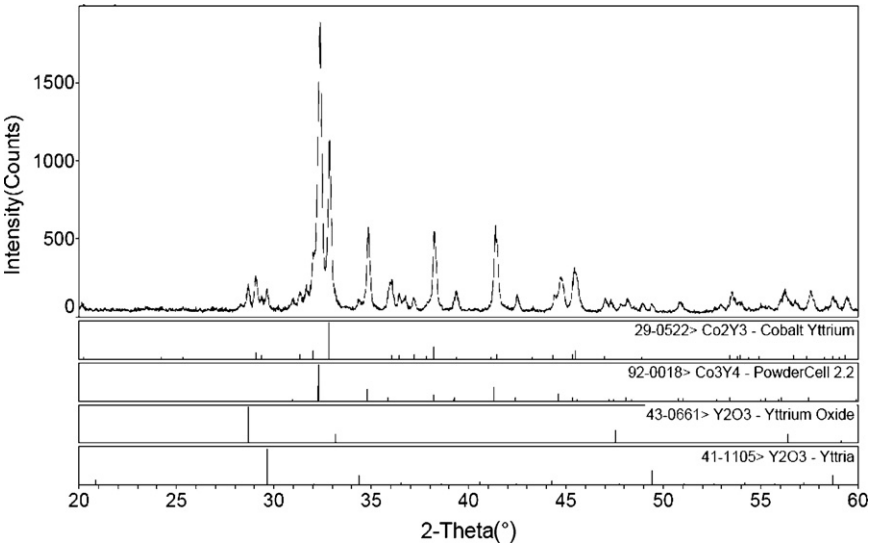

Fig. 3. XRD pattern of the sample no. 35 ($Co_{40}Y_{60}$) consisting of the phases of Y_4Co_3 and Y_3Co_2.

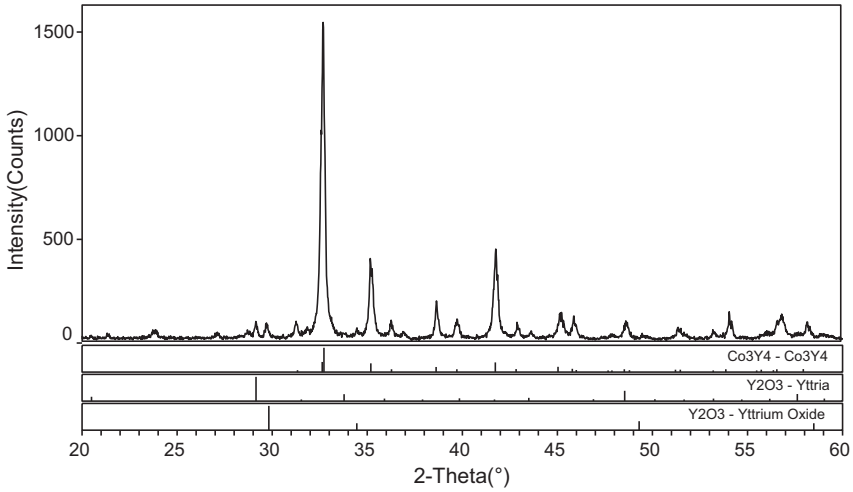

Fig. 4. XRD pattern of the sample ($Co_{42.9}Er_{30}Y_{27.1}$) consists of the single phase of $Er_{4-x}Y_xCo_3$ (the sample contained small amount of Y_2O_3).

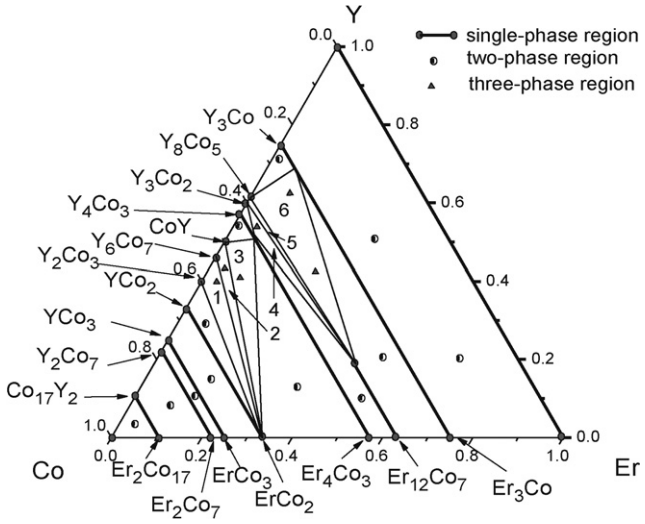

Fig. 5. The isothermal section of the Co–Er–Y ternary system at 500 °C.

temperature is between the previous measured values (750 °C in Buschow [16] and 830 °C in Wu et al. [3]). The thermal stability of $Y_{1-x}Er_xCo_5$ is discussed in another paper.

In order to verify the existence of the compound Y_3Co_2 at 500 °C, three samples with the compositions near Y_3Co_2 were prepared. Fig. 3 presents the XRD pattern of the sample no. 35 ($Co_{40}Y_{60}$) indicating that the sample contained the phases of Y_4Co_3 and Y_3Co_2 (the sample contained a little amount of Y_2O_3). The result means that the phase Y_3Co_2 exists at 500 °C under our experiment condition, which is in agreement with Wu et al. [3].

No new ternary compound was found in all binary and ternary alloy samples.

Table 1
Details of typical alloy compositions and phase components in three-phase regions.

Phase regions	Phase components	Alloy compositions
1	$Y_2Co_3 + Y_6Co_7 + ErCo_2$	No. B44 ($Co_{56}Er_3Y_{41}$)
		No. B27 ($Co_{60}Er_5Y_{35}$)
2	$Y_6Co_7 + YCo + ErCo_2$	No. B71 ($Co_{53}Er_2Y_{45}$)
		No. B42 ($Co_{55}Er_5Y_{40}$)
3	$YCo + Er_{4-x}Y_xCo_3$	No. B24 ($Co_{50}Er_4Y_{46}$)
	($x = 0.49$) + $ErCo_2$	No. 65 ($Co_{50}Er_{10}Y_{40}$)
4	$Er_{12-x}Y_xCo_7$	No. 55 ($Co_{40}Er_{10}Y_{50}$)
	($x = 3.6$) + $Er_{4-x}Y_xCo_3$	No. B72 ($Co_{41}Er_4Y_{55}$)
	($x = 0.42$) + Y_3Co_2	No. B73 ($Co_{41}Er_6Y_{53}$)
5	$Er_{12-x}Y_xCo_7$ ($x = 3.6$) + $Y_8Co_5 + Y_3Co_2$	–
6	$Er_{12-x}Y_xCo_7$ ($x = 3.6$) +	No. 68 ($Co_{35}Er_{15}Y_{50}$)
	$Y_8Co_5 + Er_{3-x}Y_xCo$ ($x = 0.24$)	No. B17 ($Co_{31}Er_8Y_{61}$)

3.2. Solid solubility

Six pairs of corresponding compounds in the Y–Co and Er–Co binary systems, i.e., Er_2Co_{17} and Y_2Co_{17}, Er_2Co_7 and Y_2Co_7, $ErCo_3$ and YCo_3, $ErCo_2$ and YCo_2, Er_4Co_3 and Y_4Co_3, Er_3Co and Y_3Co form continuous series of solid solutions because these pairs of compounds have the same space groups and the same crystal structure, almost the same lattice parameters and similar characters, respectively. Fig. 4 presents the XRD pattern of the sample with composition of $Co_{42.9}Er_{30}Y_{27.1}$ consists of the single phase of $Er_{4-x}Y_xCo_3$ (the sample contained a little amount of Y_2O_3). At the same time, metals Y and Er can substitute for each other and form substitution solid solutions.

The maximum solid solubility of Y in the compound $Er_{12}Co_7$ was determined by X-ray diffraction technique using the phase disappearing method and the scanning electron microscopy with energy dispersive analysis. With increasing the Er content, the XRD patterns of the compounds $Er_{12-x}Y_xCo_7$ were not changed but moved towards higher angle indicating that the phase has a wide solubility range because of the difference between the

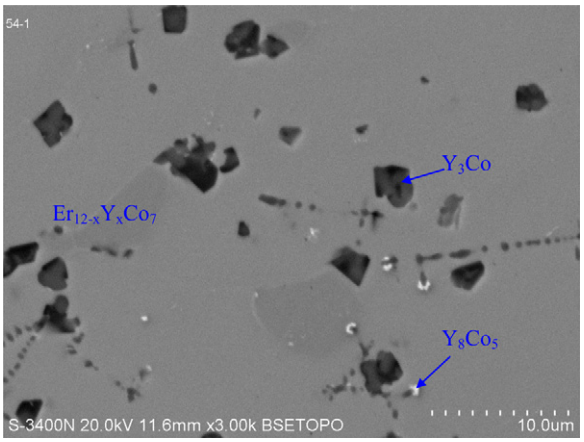

Fig. 6. Micrograph (3000×) of sample no. 54 ($Co_{35}Er_{35}Y_{30}$) in the three-phase region of $Er_{12-x}Y_xCo_7$ ($x = 3.6$) + Y_8Co_5 + $Er_{3-x}Y_xCo$ ($x = 0.24$). The gray background is the phase $Er_{12-x}Y_xCo_7$, the black pieces are $Er_{3-x}Y_xCo$ and the white ones are Y_8Co_5.

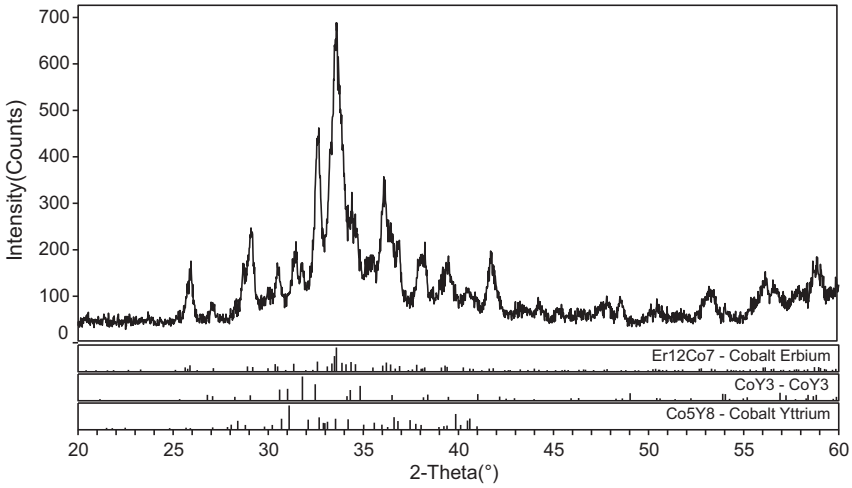

Fig. 7. XRD patterns of the sample no. 54 ($Co_{35}Er_{35}Y_{30}$) consisted of the three phases of $Er_{12-x}Y_xCo_7$ ($x = 3.6$), Y_8Co_5 and $Er_{3-x}Y_xCo$ ($x = 0.24$).

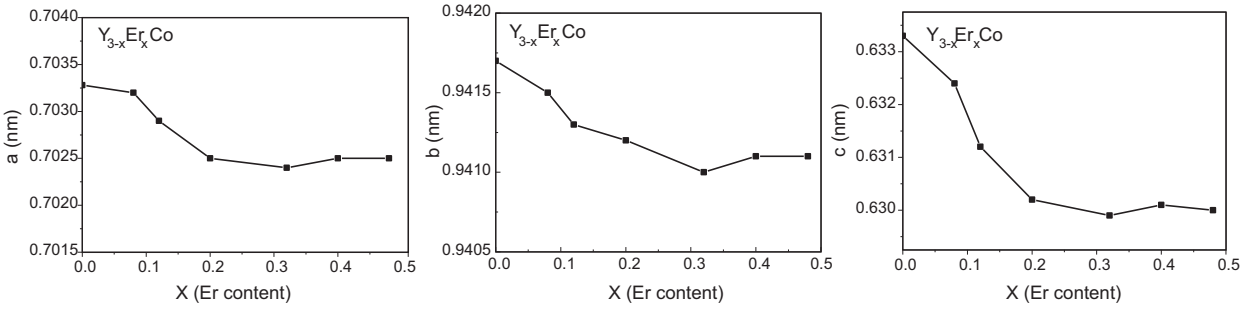

Fig. 8. The variation of lattice parameters on the Er content for $Er_xY_{3-x}Co$.

atomic radius of the Er atom and the Y atom. By comparing the movement and the disappearance of the diffraction patterns of the single phase $Er_{12-x}Y_xCo_7$ in the samples and combining with the results of SEM (EDS), the maximum solid solubility of Y in the compound $Er_{12}Co_7$ was obtained. The maximum solid solubility of Y in the compound $Er_{12}Co_7$ is about 19 at.% Y. No solid solubilities of Er in the compounds Y_2Co_3, Y_6Co_7, YCo, Y_3Co_2 and Y_8Co_5 were observed.

3.3. Isothermal section of the Co–Er–Y system at 500 °C

The isothermal section of the phase diagram of the Co–Er–Y ternary system at 500 °C was investigated by the means of X-ray powder diffraction, differential thermal analysis, scanning electron microscopy with energy dispersive analysis and optical microscopy. By comparing and analyzing a total of 160 binary and ternary alloy samples and identifying the phases in each sample,

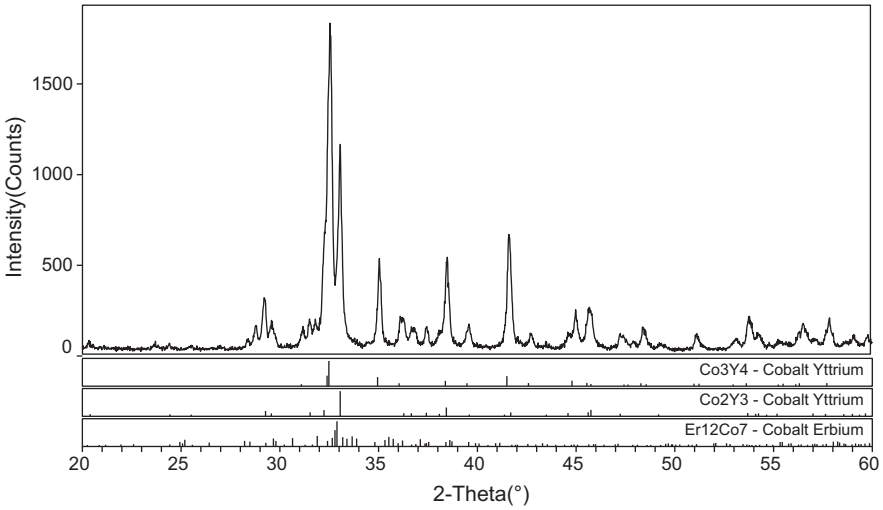

Fig. 9. XRD patterns of the sample no. 55 ($Co_{40}Er_{10}Y_{50}$) consisted of the three phases of $Er_{4-x}Y_xCo_3$ ($x = 0.42$), Y_3Co_2 and $Er_{12-x}Y_xCo_7$ ($x = 3.6$).

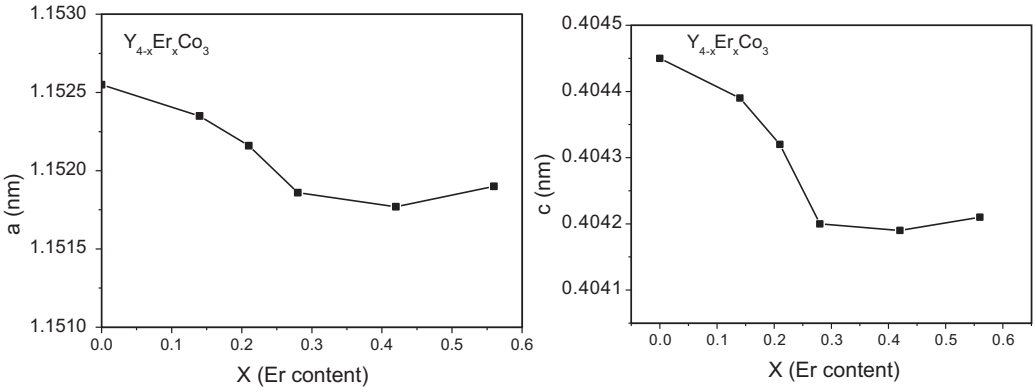

Fig. 10. The variation of lattice parameters on the Er content for $Er_xY_{4-x}Co_3$.

the 500 °C isothermal section of the phase diagram of the Co–Er–Y ternary system is determined. The isothermal section consists of 14 single-phase regions, 19 two-phase regions, and 6 three-phase regions, as shown in Fig. 5. Table 1 presents the details of the three-phase regions of the isothermal section of the ternary Co–Er–Y system and the typical alloy compositions. Fig. 6 presents the SEM micrograph of the sample no. 54 ($Co_{35}Er_{35}Y_{30}$) in the three-phase region of $Er_{12-x}Y_xCo_7$ ($x = 3.6$) + Y_8Co_5 + $Er_{3-x}Y_xCo$ ($x = 0.24$). The gray background with measured composition of $Co_{34.5}Er_{46.3}Y_{19.2}$ is the phase $Er_{12-x}Y_xCo_7$ ($x = 3.6$), the black pieces with measure composition of $Co_{26.5}Er_{6.3}Y_{67.2}$ are $Er_{3-x}Y_xCo$ ($x = 0.24$) and the white ones are Y_8Co_5 (with measured composition of $Co_{36.5}Er_{0.4}Y_{63.1}$). The XRD pattern of the same sample no. 54 ($Co_{35}Er_{35}Y_{30}$) is given in Fig. 7 indicating the co-existence of three-phases of $Er_{12-x}Y_xCo_7$ ($x = 3.6$), Y_8Co_5 and $Er_{3-x}Y_xCo$ ($x = 0.24$). Fig. 8 shows the variation of the lattice parameters on the Er content for $Er_xY_{3-x}Co$ in the samples with composition of 70 at.% Co in the range from 0 to 12 at.% Er ($x = 0$–0.48). Fig. 9 presents the XRD pattern of the sample no. 55 ($Co_{40}Er_{10}Y_{50}$) consisting of the three phases of $Er_{4-x}Y_xCo_3$, Y_3Co_2 and $Er_{12-x}Y_xCo_7$ showing the existence of the three-phase region of $Er_{4-x}Y_xCo_3$ ($x = 0.42$) + Y_3Co_2 + $Er_{12-x}Y_xCo_7$ ($x = 3.6$). Fig. 10 shows the variation of the lattice parameters on the Er content for $Er_xY_{4-x}Co_3$ in the samples with composition of 41.5 at.% Co in the range from 0 to 8 at.% Er ($x = 0$–0.56).

4. Conclusion

The isothermal section of the phase diagram of the Co–Er–Y ternary system at 500 °C was determined. The isothermal section consists of 14 single-phase regions, 19 two-phase regions and 6 three-phase regions. Six pairs of corresponding compounds, i.e., Er_2Co_{17} and Y_2Co_{17}, Er_2Co_7 and Y_2Co_7, $ErCo_3$ and YCo_3, $ErCo_2$ and YCo_2, Er_4Co_3 and Y_4Co_3, Er_3Co and Y_3Co form continuous series of solid solutions. The maximum solid solubility of Y in the compounds $Er_{12}Co_7$ is about 19 at.% Y. No solid solubilities of Er in the compounds Y_2Co_3, Y_6Co_7, YCo, Y_3Co_2 and Y_8Co_5 were observed. The binary compounds YCo_5 and $ErCo_5$ were not observed at 500 °C. No new ternary compound was found.

Acknowledgements

This work was supported by the Natural Science Foundation of China (nos. 50861005 and 50961002), the Graduate Innovative Projects of Guangxi (no. 105930903002) and Natural Science Foundation of Guangxi (no. 0832027).

References

[1] T.B. Massalski, H. Okamoto, P.R. Subramanian, L. Kacprzak (Eds.), Binary Alloy Phase Diagrams, 2nd ed., ASM, 1990.
[2] K.H.J. Buschow, Philips Res. Rep. 26 (1971) 49–64.
[3] C.H. Wu, Y.C. Chuang, X.P. Su, Z. Metallkde. 82 (H. 1) (1991) 73–79.
[4] C.H. Wu, Y.C. Chuang, J. Phase Equilib. 12 (5) (1991) 587–592.
[5] Z. Du, D. Lu, J. Alloys Compd. 373 (2004) 171–178.
[6] K.H.J. Buschow, J. Less-Common Met. 37 (1) (1974) 91.
[7] K.H.J. Buschow, Rep. Prog. Phys. 40 (1977) 1179.
[8] A.E. Ray, Cobalt Cobalt Abstr. 1 (1974) 13.
[9] A.K. Grover, B.R. Coles, B.V.B. Sarkissian, H.E.N. Stone, J. Less-Common Met. 86 (1982) 29.
[10] L. Zeng, W. He, Y. Zhuang, Z. Metallkd. 89 (4) (1998) 286.
[11] L. Zeng, J. Liang, Y. Zhuang, J. Alloys Compd. 256 (1–2) (1997) 228–229.
[12] Y.H. Zhuang, Q.M. Zhu, J.Q. Li, et al., J. Alloys Compd. 422 (2006) 214–217.
[13] X. Chen, Y.H. Zhuang, J.L. Yan, F. Fei, J. Alloys Compd. 479 (1–2) (2009) 35–38.
[14] W. He, L. Tang, L. Yang, et al., J. Alloys Compd. 491 (2010) 149–152.
[15] Materials Data JADE Release 5, XRD Pattern Processing, Materials Data Inc. (MDI), 1999.
[16] K.H.J. Buschow, J. Less-Common Met. 31 (3) (1973) 359.